Experimental and theoretical study of nanofiltration of weak electrolytes: $SO_4^{2-}/HSO_4^-/H^+$ system

Julio López[a*], Mònica Reig[a], Andriy Yaroshchuk[a,b], Edxon Licon[a], Oriol Gibert[a,c], José Luis Cortina[a,c]

[a] *Chemical Engineering Department (UPC-BarcelonaTECH) and Barcelona Research Center for Multiscale Science and Engineering, C/ Eduard Maristany, 10-14 (Campus Diagonal-Besòs), E-08930 Barcelona, Spain*

[b] *Catalan Institute for Research and Advanced Studies (ICREA), Barcelona, Spain*

[c] *Water Technology Center CETaqua, Carretera d'Esplugues 75, E-08940 Cornellà de Llobregat, Spain*

[*] julio.lopez.rodriguez@upc.edu

Abstract

Over recent years, nanofiltration (NF) has been considered as an effective way to improve processing steps in metallurgical and hydrometallurgy applications dealing with mixtures of metal ions in sulphuric-acid-dominated solutions. The principal advantage of NF membranes over reverse osmosis (RO) membranes is their ability to allow for a practically free passage of acid, while metallic species, especially multi-charged species, are efficiently rejected. In general, these sulphuric solutions cover a range from strongly acidic solutions with pH below 1 up to moderately acidic solutions of pH 3. Over this range, changes in the feed acidity influence both the aqueous electrolyte solution speciation ($SO_4^{2-}/HSO_4^-/H^+$) and the membrane acid–base properties (protonation of carboxylic and amine groups). However, few studies have been published on the trans-membrane transport of inorganic species coupled to changes in their speciation as well as to the properties of the membrane phase.

In this study, experimental data on the sulphuric acid rejection for pH values from 1 to 3 have been obtained with an aromatic poly(piperazine)amide membrane (NF270) at various trans-membrane pressures. The results were modelled by a novel version of the Solution-Electro-Diffusion model taking into account equilibrium reactions, and a general (quasi)analytical solution was obtained for the transport of weak electrolytes of arbitrary valence type. The equilibrium weak acid reaction made the total sulphate (SO_4^{2-}/HSO_4^-) rejection decrease strongly as the fraction of single-charged hydrogen sulphate (HSO_4^-) in the feed increased. From the modelling procedure, permeances to H^+, HSO_4^- and SO_4^{2-} over the studied pH range were determined.

Key words

Reactive transport, modelling, ionic permeances, NF270, sulphuric acid

1. Introduction

Sulphuric acid is one of the most produced chemicals worldwide. In the past the scale of its production was even used as an indicator of industrial strength. Nowadays, sulphuric acid is still widely used in a large number of applications (e.g. mineral processing, hydrometallurgy and for pH control). In the mining industry, it is used as a leaching agent to dissolve minerals

for metal extraction [1]; sulphuric acid is also used in electroplating and acid pickling in the metal-finishing industry [2]. In both cases, a large amount of effluent is generated. However, new environmental legislation promotes sustainability and sulphuric acid recovering technologies. Therefore, as an alternative to neutralisation/precipitation, several techniques, such as electrolytic deposition, ion exchange, diffusion dialysis, electrodialysis, solvent extraction [2–5] and more recently pressure-driven membrane processes, have been applied to treat these effluents. Among them, nanofiltration (NF) offers unique opportunities for acid purification. Typically, NF membranes show low rejection of acids, but high rejection of multivalent ions. As the acid rejection is low, its concentrations on both sides of the membrane are close to each other. Accordingly, the contribution of acid to the differential osmotic pressure is very limited [6]. Then, in comparison with the techniques listed above, it has relatively low energy consumption.

The use of NF for removing metal ions from acidic solutions has been previously studied [7–13]. Nÿstrom et al. [10] separated metal (iron, chromium and nickel) sulphates and nitrates from acidic media achieving high rejections (around 99%) with an NF-45 membrane. González et al. [12] tested several reverse osmosis(RO and NF membranes in the treatment of concentrated phosphoric streams (from 2 to 8 M). NF allowed to obtain higher flows and higher acid permeations than did RO. However, the metal rejection in RO was a little higher than in NF. Skidmore and Hutter [13] patented a process for purification of phosphoric acid by NF. High rejections of multivalent ions (Al(III), Fe(III), Mg(II)) were observed. Thus, the typically high ion concentration of strongly acidic solutions, which may restrict the use of other membrane techniques, can be overcome with nanofiltration.

Modelling of ion rejection in NF is useful for the process optimisation and scale-up. Ion transport through NF membranes has been widely described by either non-equilibrium thermodynamic models [14–17] or extended Nernst–Planck equations [18–21]. Among various approaches, Yaroshchuk et al. [22] demonstrated that, for single salts, the Solution-Diffusion-Film (SDF) model is applicable, and later it was extended to electrolyte mixtures by including the coupling between the electro-diffusion fluxes of various ions via the electric field of the membrane potential [23–25]. Taking this into account, a good description of ion rejection dependence on the trans-membrane volume flow was achieved for a number of electrolyte mixtures consisting of one dominant salt and trace ions [24,25]. This approach also accounts for the existence of a concentration-polarisation layer where the ion transfer occurs via electro-diffusion and convection. This description of trans-membrane mass transfer by the so-called Solution-Electro-Diffusion-Film (SEDF) model allows for efficient determination of membrane permeances to single ions from experimental data. However, to date only limited attempts have been reported to describe membrane transport of solutes being in chemical equilibrium with other solutes (e.g. anions with acid/base properties, or ions with complexing properties) [7,26]. This is the case with the sulphuric acid solutions where, at pH values close to the pK, HSO_4^- and SO_4^{2-} species are present in commeasurable concentrations. In order to model these results, the equilibrium reaction must be accounted for in the model. By using the solution–diffusion model, Nir. et al. [27,28] considered proton and hydroxyl ions as traces in RO, taking into account the chemical equilibrium between them. Niewersch et al. [29,30] modelled numerically the trans-membrane ion fluxes under high-acidity conditions in NF. In this paper we present a novel quasi-analytical approach to the modelling of NF transport in a

system of three components, coupled by an equilibrium chemical reaction. For simplicity, in this study we neglected the concentration polarisation phenomena in the first approximation.

Another objective of this work is to extending the validation of the SEDF model towards the transport of reacting species via comparison with experiment. A wide pH range was used in order to explore the effect of changes in the acid–base equilibrium of the membrane functional groups, and to evaluate the effect of incomplete acid dissociation. The experiments were carried out using an NF270 membrane in a cross-flow experimental set-up. The results of these measurements have been interpreted in terms of ionic permeances of the membrane to HSO_4^-, SO_4^{2-} and H^+.

2. Reactive transport of ions in nanofiltration membranes: model formulation

The ion fluxes are described according to the Solution-Electro-Diffusion model. One of the assumptions of this model is that there is no coupling between solute and solvent flows inside the membrane or, in other words, reflection coefficients are assumed to be equal to one for all species. The model uses 'virtual' concentrations, which are defined as those in a solution that could be in thermodynamic equilibrium with an infinitely small volume inside the membrane. 'Virtual' concentrations satisfy the chemical-equilibrium condition with the bulk association constant. The partitioning coefficients, which quantify the ratios between the real and virtual species concentrations in the membrane (and possible changes of association constant there) are included in the ion permeances [24]. The ion transport is described by Eq 1.

$$j_i = -P_i \cdot c_i \cdot \left(\frac{dln\, c_i}{dx} + z_i \cdot \frac{d\varphi}{dx}\right) \quad (1)$$

where j_i (mol/m^{2}s) is the trans-membrane volume flow of component I; P_i is the membrane permeability to ion i; c_i and z_i stand for its virtual concentration and its charge, respectively; φ is the dimensionless virtual electrostatic potential and x is the position across the membrane.

The transport of ions is:

- Subjected to the zero-current condition defined by Eq. 2.

$$\sum_i z_i \cdot j_i = 0 \quad (2)$$

- Subjected to the electro-neutrality condition in the virtual solution defined by Eq. 3:

$$\sum_i z_i \cdot c_i = 0 \quad (3)$$

- Virtual ion concentrations are not independent but related by a chemical equilibrium condition at a given constant temperature and ionic strength ($\alpha = 10^{pK_a}$), where pK_a is the acidity constant, defined by Eq. 4:

$$c_3 = \alpha \cdot c_1 \cdot c_2 \quad (4)$$

115 It should be stressed that the chemical reaction is subjected to charge conservation
116 ($z_3 = z_1 + z_2$)

117 By using Eqs. 1 and 2 for a system of three ions (e.g. H^+, HSO_4^-, SO_4^{2-}) an expression for the
118 gradient of electrostatic potential in virtual solution can be derived (Eq. 5):

$$\frac{d\varphi}{dx} = -\sum_i \left(\frac{t_i}{z_i}\right) \cdot \frac{dln\ c_i}{dx} \tag{5}$$

119

120 where t_i is the transport number of ion 'i' defined by Eq. 6:

$$t_i = \frac{z_i^2 \cdot P_i \cdot c_i}{\sum_j z_j^2 \cdot P_j \cdot c_j} \tag{6}$$

121

122 From the chemical equilibrium condition, a relationship can be obtained between the
123 derivatives of logarithms of concentrations of the species described by Eq. 7:

$$\frac{dln\ c_3}{dx} = \frac{dln\ c_1}{dx} + \frac{dln\ c_2}{dx} \tag{7}$$

124

125 By combining the chemical equilibrium and electro-neutrality conditions (in the virtual
126 solution) we obtain this:

$$\frac{dln\ c_2}{dx} = \frac{1}{1 + \alpha \cdot \left(1 + \frac{z_1}{z_2}\right) \cdot c_1} \cdot \frac{dln\ c_1}{dx} \tag{8}$$

127

128 Due to the chemical reaction, the trans-membrane ion fluxes of all three components are not
129 conservative (they change across the membrane). However, owing to the reaction
130 stoichiometry, exactly the same amount of species '1' and '2' is consumed (produced) at a
131 given point inside the membrane. Therefore, the difference in their fluxes is constant and
132 equal to the product of trans-membrane volume fluxes and difference of their concentrations
133 in the permeate. By using this, as well as Eqs. 5,7 and 8 it is possible to formulate just one
134 transport equation in terms of concentration of only one of the species (for example, species
135 '1'). In this equation, the variables (concentration of species '1' and space variable) can be
136 separated so the equation can be solved in quadrature, and after some identical
137 transformations, this could be obtained:

$$J_v L = \frac{\int_{c_{1p}}^{c_{1f}} F(c_1) dc_1}{c_{1p} \cdot \left(1 + \frac{z_1}{c_{1p} \cdot \alpha \cdot (z_1 + z_2) + z_2}\right)} \tag{9}$$

138

139 where c_{1f}, c_{1p} are the concentrations of species '1' in the feed and permeate, respectively, L is
140 the active-layer thickness, and:

$$F(c_1) \equiv z_2 \cdot z_3 \cdot \frac{P_1 \cdot (z_2 + c_1 \cdot \alpha \cdot z_3) \cdot (P_2 + P_3 \cdot \alpha \cdot c_1) - P_2 \cdot P_3 \cdot z_1 \cdot \alpha \cdot c_1}{z_2 \cdot (P_2 \cdot z_2 - P_1 \cdot z_1) + c_1 \cdot \alpha \cdot z_3 \cdot (P_3 \cdot z_3 - P_1 \cdot z_1)} \cdot \frac{z_2 + c \cdot \alpha \cdot z_3 - z_1}{(z_2 + c_1 \cdot \alpha \cdot z_3)} \tag{10}$$

This general expression (Eq. 9) is valid for any weak electrolyte. A detailed derivation of Eq. 9 is presented in Annex 1.

In principle, the integral in Eq. 9 can be taken analytically but the corresponding expression is too cumbersome to be shown here. Nonetheless, the availability of the relatively simple expression of Eq. 9 enables us to verify the solution by considering the limiting cases of no reaction ($\alpha = 0$) and dominant reaction ($\alpha \to \infty$). In both limiting cases, the integrand is independent of concentration, so the integral can be easily, taken to obtain:

$$\frac{c_{1f}}{c_{1p}} = 1 + \frac{J_v L}{P_{12}} \qquad \text{at } \alpha = 0 \tag{11}$$

$$\frac{c_{1f}}{c_{1p}} = 1 + \frac{J_v L}{P_{13}} \qquad \text{at } \alpha \to \infty \tag{12}$$

where it was denoted

$$P_{12} \equiv \frac{(z_1 - z_2) \cdot P_1 P_2}{z_1 P_1 - z_2 P_2} \qquad P_{13} \equiv \frac{(z_1 - z_3) \cdot P_1 P_3}{z_1 P_1 - z_3 P_3} \tag{13}$$

It is easy to see that Eqs. 11 and 12 are just expressions (within the scope of the solution–diffusion model with negligible concentration polarisation) of the reciprocal transmission of either of two single salts consisting of ions '1' and '2' ($\alpha = 0$) or '1' and '3' ($\alpha \to \infty$), P_{12} and P_{13} being the corresponding salt permeabilities. Thus, the solution of Eq. 9 is in agreement with these two limiting cases. One can also see that though Eq. 9 is transcendental in c_{1p} it provides an explicit dependence of trans-membrane volume flow on the permeate concentration. This dependence can readily be used for the analysis of dependence of rejection on the trans-membrane volume flow.

If it is further assumed that $P_3 > P_2$, which is naturally due to the smaller charge magnitude of ion '3', one can show the integrand in the right-hand side of Eq. 9 to increase with the virtual concentration in a monotonic way. Interestingly, this does not mean that the rejection of weak electrolyte decreases monotonically with its feed concentration. Actually, due to the presence of the denominator in the right-hand side of Eq. 9, there is a slight minimum on the dependence of rejection (at a given trans-membrane volume flow) on the feed concentration (or association constant). This is illustrated by the results of some sample calculations shown in Figure 1.

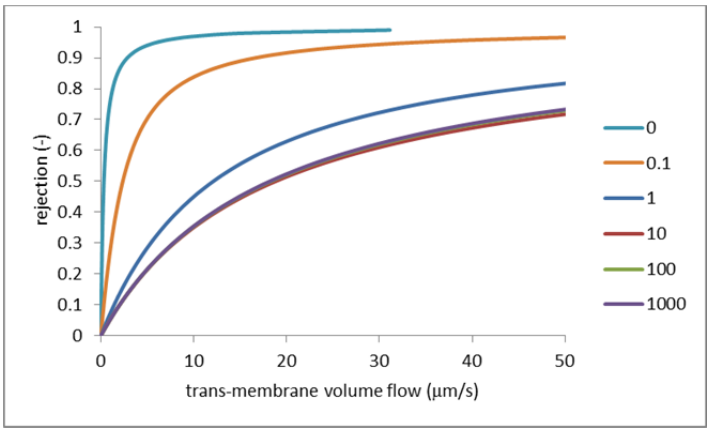

Figure 1. Dependence of rejection of ion '1' on trans-membrane volume flow for various association constants

One can see that initially the rejection decreases strongly with increasing product of feed concentration and chemical equilibrium dissociation constant. However, starting from $\alpha \cdot c_{1f} \approx 10$ there is practically no visible dependence. Below, we will see that this levelling out at higher concentrations is in agreement with our experimental data.

In this study, NF rejections of sulphuric acid at various feed acidities (concentrations) using a semi-aromatic polyamide NF membrane (NF270) were investigated experimentally. The observable rejections (R_{obs}) of the acid were calculated by using Eq. 14:

$$R_{obs} = 1 - \frac{C_p}{C_f} \tag{14}$$

where C_p and C_f are the concentrations of acid in the permeate and feed of the membrane experimental setup, respectively.

Eq. 9 was used to fit experimental data on the total sulphate rejection via determining a set of three ion permeances ($SO_4^{2-}/HSO_4^-/H^+$). The permeances are defined as the permeabilities divided by the barrier-layer thickness. From Eq. 9, one can see that just these quantities can be fitted to experimental data provided that the barrier-layer thickness is not specified.

The integral in the right-hand side of Eq.9 was calculated numerically. In Figure 1 a flow chart of the algorithm used is shown. The algorithm was implemented with Matlab® using the function *fminsearch* (based on Nelder–Mead algorithm) to reach converge criteria and the function *quad* to take the integral.

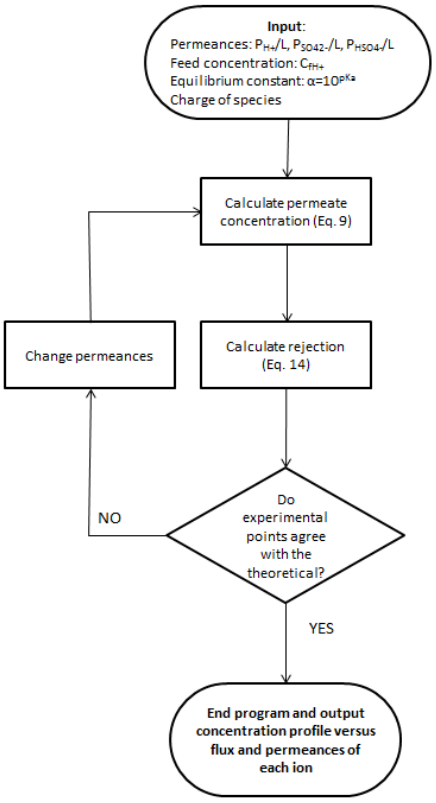

188

189 **Figure 2. Details on the Matlab® implemented algorithm**

190 The objective function (OF) (Eq. 15) was used to minimise the relative error between the
191 measured and predicted permeate ion concentrations:

$$O.F. = \sum \frac{|C_{p_{model}} - C_{p_{experimental}}|}{C_{p_{experimental}}} \quad (15)$$

192 # 3. Experimental section

193 ## 3.1. Membranes, reagents and solutions

194 We used an NF membrane with active layer of semi-aromatic poly(piperazine) amide (NF270,
195 Dow Chemical). Its chemical structure is shown in Figure 3.

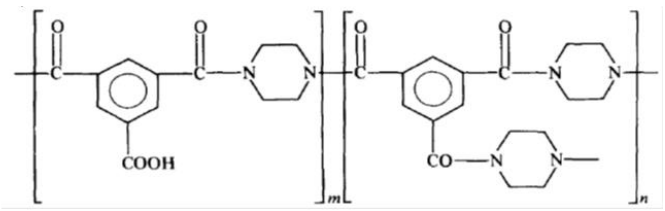

196

197 **Figure 3. Chemical structure of the membrane active layer [31,32]**

198 Aromatic polyamide active layers prepared via interfacial polymerisation as in NF90 or ESNANF
199 membranes (similarly to NF270) have been characterised in terms of concentration of
200 ionisable functional groups (carboxylic (RCOOH/R–COO^-) and amine (R–NH_3^+/R–NH_2)) related

to the degree of polymer cross-linking [33,34]. These membranes have isoelectric points (IEPs) of 3.5 and 4.3, respectively, which are very close to the isoelectric point of NF270 [35]. Although no data on the acidity constants of the carboxylic groups have been published, most of the characterisation studies on the acid–base properties concluded that at pH values lower than 3, carboxylic groups are protonated (R–COOH) and at pH values above 5 they are deprotonated ($R–COO^-$). Thus, in the present study the experiments were performed at pH values supposedly below the isoelectric point so the carboxylic groups were protonated [36], even though, at lower pH than the IEP, membrane was positively charged due to the presence of protonated amine groups ($R–NH_3^+$).

The experiments were carried out using sulphuric acid supplied by Sigma-Aldrich (95–97 wt%). The pH of the feed solutions in our experiments lay between 3 and 1. In this pH range the mono-charged sulphate species (hydrogen sulphate, HSO_4^-) was present in solution in noticeable amounts (Figure 4, [37]).

3.2. Membrane cross-flow experimental setup

We used an experimental setup as previously described[38]. Experiments were performed with NF270 membrane (0.014 m^2) in a cross-flow set-up equipped with a test cell (GE SEPA^{TM} CF II) with a spacer-filled feed channel. In this setup the cross-flow velocity (cfv) and trans-membrane pressure (TMP) could be adjusted independently.

Feed working solutions were kept at constant temperature (21 ± 2 °C) in a thermostated 30 L feed tank and pumped into the cross-flow filtration system with a high-pressure diaphragm pump (Hydra-Cell, USA) at prefixed cross-flow velocities (cfv) and trans-membrane pressures. The two output streams from the test cell, permeate and concentrate, were recirculated through stainless steel pipes into the feed tank, thus providing a fairly constant concentration in the feed solution. At a given cfv the TMP could be varied by a needle valve located in the concentrate stream just at the exit from the test cell. The concentrate passed through a manometer and a flow meter. A pre-filter cartridge was placed in the concentrate loop to eliminate corrosion products and microorganisms. A major part of the permeate stream was recycled back to the feed tank, and permeate samples for analysis were collected via a three-way valve.

Prior to the measurements, the membranes were held in deionised water overnight to remove conservation products. Then, the membrane was compacted with deionised water at 22 bar and 1 m/s cfv. Before the experiments, the membrane was additionally compacted with the feed solution at 22 bar and cfv of 1 m/s for 2 h. The experiment was performed at fixed cross-flow velocity (0.7 m/s) and the TMP was varied.

The system is equipped with flow meters, pressure meters, a conductivity meter (Crison GLP 31 EC), a pH meter (Crison GLP 21) and a temperature sensor, to monitor the hydrodynamic and chemical parameters. Furthermore, a data acquisition system programmed in LABVIEW® version 8.6 (Laboratory Virtual Instrumentation Engineering Workbench) was developed. Sensor calibrations were performed under the hydrodynamic conditions used in the experimental work.

3.3. Ion rejection experimental tests with H_2SO_4 solutions

Aqueous solutions of H_2SO_4 were used as feed solutions. These selected model solutions reproduced some common scenarios of acidity of mining and metallurgical process waters. HYDRA-MEDUSA software was used to evaluate the dissociation of sulphuric acid [37]. The experiments were performed with feed solutions having pH values between 1 and 3. The speciation of H^+, SO_4^{2-} and HSO_4^- species is shown in Figure 4. It can be seen that the experiments covered the range from below the pKa of the SO_4^{2-}/HSO_4^- equilibrium, where HSO_4^- was the dominant species, up to values above the pKa, where SO_4^{2-} was dominant.

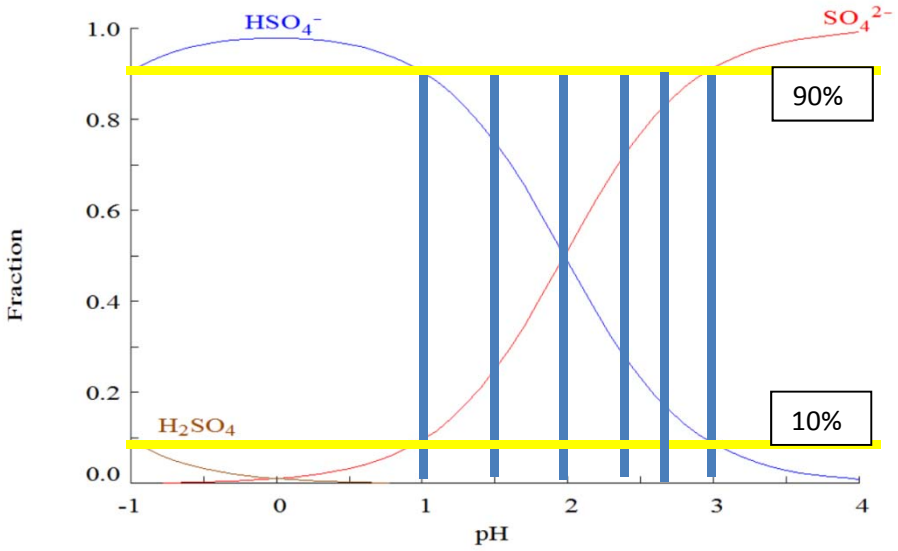

Figure 4. Variation of the H_2SO_4/ HSO_4^-/SO_4^{2-} molar fractions as a function of pH by using the equilibrium code Medusa and using the thermodynamic data from the Hydra database (Hydra) [37]. Vertical blue lines represent the pH values of the experiments carried out.

As can be seen in Figure 4, in the studied pH range the presence of H_2SO_4 as species can be disregarded as it is present only at pH values below –1 (e.g. $C_{H2SO4} > 5$ M).

Total concentration of sulphuric acid in the feed solutions varied between 0.5 and 50 mmol/L. The details of experimental conditions are summarised in Table 1. Feed solution pH was adjusted to the values shown in Table 1.

Table 1. Experimental conditions for the transport of multi-ion solutions of H_2SO_4 by the NF270 membrane at 21 ± 1 °C.

Feed concentration		Cross-flow velocity	Trans-membrane pressure
$C^o(H_2SO_4$(mol/L))	pH^o	(m/s)	(bar)
5 x 10^{-2}	1	0.7	4.0–14
1.6 x 10^{-2}	1.5	0.7	4.0–14
5 x 10^{-3}	2	0.7	4.0–14
2 x 10^{-3}	2.3	0.7	4.0–14
9 x 10^{-4}	2.7	0.7	4.0–14
5 x 10^{-4}	3	0.7	4.0–14

The trans-membrane volume flow (J_v) was determined by monitoring the collected permeate volume. Ion concentrations in feed and permeate samples were measured by ion chromatography (Dionex ICS-1000). Total sulphate concentrations were analysed by using the IONPAC® AS23 anion-exchange column using a mixture of 45 mM Na_2CO_3 and 0.8 mM $NaHCO_3$ as eluent solution. The pH of the feed and permeate solutions were measured with a pH electrode.

Measured total sulphate concentrations $[SO_4^{2-}/HSO_4^-]_t$ and proton activities:

$$pH = -\log\left(a(H^+)\right) = -\log\left([H^+]\cdot\gamma'(H^+)\right) \quad (16)$$

were compared when necessary with those predicted by using HYDRA-MEDUSA code. Concentration values of ionic species in solution (H^+, HSO_4^-, SO_4^{2-}) were calculated taking into account the weak-acid equilibrium (Eq. 17):

$$H^+ + SO_4^{2-} \leftrightarrow HSO_4^- \qquad \log\alpha\ (21\ °C) = 1.98 \quad (17)$$

and the mass and electroneutrality balances (Eqs. 18-21):

$$[SO_4^{2-}/HSO_4^-]_t = [SO_4^{2-}] + [HSO_4^-] \quad (18)$$

$$[HSO_4^-] = \alpha\cdot[H^+]\cdot[SO_4^{2-}] \quad (19)$$

$$[SO_4^{2-}] = \frac{[SO_4^{2-}/HSO_4^-]_t}{[1 + H^+\cdot\alpha]} \quad (20)$$

$$[H^+] = 2\cdot[SO_4^{2-}] + [HSO_4^-] \quad (21)$$

From the general expression (Eq. 9), and taking the species 1, 2 and 3 as H^+, SO_4^{2-} and HSO_4^-, respectively, the following equation will describe the flux of H^+ through the membrane for the H_2SO_4 case (Eq. 22):

$$J_v L = \frac{\int_{c_{H^+p}}^{c_{H^+f}} F(c_{H^+}) dc_{H^+}}{c_{H^+p} \cdot \left(1 + \frac{1}{-c_{H^+p} \cdot \alpha - 2}\right)} \quad (22)$$

Where $\alpha = 10^{pK_a} = 10^{1.98}$ and

$$F(c_{H^+}) \equiv 2 \cdot \frac{P_{H^+} \cdot (-2 - c_{H^+} \cdot \alpha) \cdot \left(P_{SO_4^{2-}} + P_{HSO_4^-} \cdot \alpha \cdot c_{H^+}\right) - P_{SO_4^{2-}} \cdot P_{HSO_4^-} \cdot \alpha \cdot c_{H^+}}{-2 \cdot \left(-2 \cdot P_{SO_4^{2-}} - P_{H^+}\right) - c_{H^+} \cdot \alpha \cdot (-P_{HSO_4^-} - P_{H^+})} \cdot \frac{-2 - c_{H^+} \cdot \alpha - 1}{(-2 - c_{H^+} \cdot \alpha)} \quad (23)$$

4. Results and discussion

4.1. Sulphuric acid rejection by aromatic poly(piperazine) NF270 membrane: influence of pH on rejection

Figure 5 shows the observable rejection of total sulphate as a function of trans-membrane volume flow at various feed pH values. The symbols represent the experimental points and the lines were obtained by using the Solution-Diffusion-based model described in Section 2 (Eq. 9).

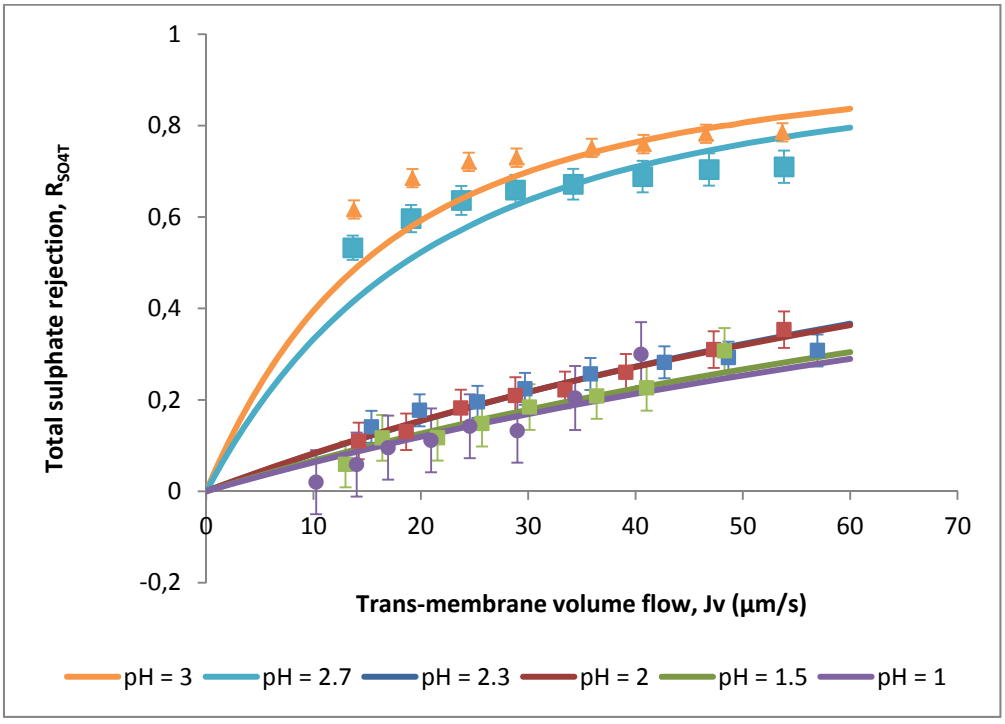

Figure 5. Total sulphate $(SO_4^{2-}/HSO_4^-)_t$ rejection in solutions at different pH values as a function of trans-membrane volume flow. Solid lines were obtained by the Solution-Electro-Diffusion model.

Table 2 collects the experimental data from the experiments, including TMP, trans-membrane flow, sulphate concentration and pH.

Table 2. Trans-membrane flow, total sulphate concentration and pH for feed and permeate in a range of TMP from 4 to 14 bar.

ΔP (bar)	Feed	4	5.5	7	8.5	10	12	14
J_v (µm/s)		13.77	19.22	24.47	28.92	35.93	40.75	46.55
$[SO_4^{2-}/HSO_4^-]$ (ppm)	59.65	22.87	18.78	16.66	16.11	14.83	14.34	13.00
pH	2.95	3.32	3.41	3.48	3.53	3.57	3.55	3.55
J_v (µm/s)		13.66	19.09	23.77	28.81	34.20	40.67	46.86
$[SO_4^{2-}/HSO_4^-]$ (ppm)	86.84	41.51	35.84	32.31	30.28	29.15	27.68	26.29
pH	2.76	3.00	3.05	3.10	3.13	3.14	3.17	3.17
J_v (µm/s)		15.40	19.88	25.28	29.70	35.80	42.70	48.66
$[SO_4^{2-}/HSO_4^-]$ (ppm)	274.93	236.18	226.24	221.15	213.31	204.36	197.37	194.57
pH	2.36	2.39	2.41	2.43	2.43	2.45	2.46	2.46
J_v (µm/s)		14.21	18.63	23.72	28.80	33.43	39.10	47.29
$[SO_4^{2-}/HSO_4^-]$ (ppm)	603.33	536.92	524.79	493.36	476.96	469.59	446.29	416.31
pH	2.01	2.05	2.06	2.06	2.07	2.08	2.08	2.11
J_v (µm/s)		12.98	16.40	21.56	25.70	30.13	36.39	41.03
$[SO_4^{2-}/HSO_4^-]$ (ppm)	2462.87	2318.17	2175.28	2174.37	2098.26	2009.08	1949.15	1905.50
pH	1.52	1.54	1.55	1.57	1.57	1.58	1.60	1.60

J_v (µm/s)		10.24	14.02	16.95	20.95	24.56	28.99	34.38
[SO_4^{2-}/ HSO_4^-] (ppm)	6309.13	6182.82	5940.24	5707.34	5605.95	5411.45	5472.72	5021.21
pH	1.04	1.09	1.10	1.11	1.12	1.12	1.13	1.15

The rejections of total sulphate species (SO_4^{2-}/ HSO_4^-) increased quasi-linearly for all the experiments (apart from pH 3 and pH 2.7) up to values between 30 and 35% at the maximum achieved trans-membrane volume flow (40–50 µm/s), without reaching the typical values obtained with sulphate solutions at neutral to basic conditions (>99%) in the same range of concentrations and trans-membrane volume flows [25,38,39]. At pH 3, the total sulphate rejection reached values around 75%. It was still considerably reduced compared to the typical sulphate rejections of >99%, due to the noticeable presence of monovalent specie HSO_4^- in the feed. When pH was lowered, the amount of HSO_4^- species increased significantly, leading to lower sulphate rejections (around 35%). Given the scattering, at pH < 2.3 the total sulphate rejection was practically independent of pH, which is in agreement with the theoretical calculations above (see Fig.1).

Ion rejections can be expected to be dependent on the membrane properties, especially effective fixed charges, and on solution composition. The dependence on membrane properties is related to the ion interactions with the polymer matrix (e.g. sorption or solution of the ions into the polymer matrix) and to free functional groups (e.g. adsorption and complexation of counter-ions to the fixed charge sites of the polymer membrane matrix, which diminishes the effective fixed charge). NF270 has an isoelectric point around 3 [26,40] which makes thee membrane positively charged when pH is below the IEP. In all our experiments the pH was lower than the IEP, making the membrane charge positive, and increasing when pH was lowered. However, the low total sulphate rejection could also be primarily related to the low degree of dissociation of the acid [7]. As pH decreases, the total amount of monovalent sulphate species (hydrogen sulphate) increases and it becomes dominant in solution. This change of feed composition results in a lower rejection of total sulphate.

Among various mechanisms invoked to describe the ion rejection by NF membranes, dielectric exclusion should be taken into account. It is caused by the interactions of ions with bound electric charges induced by ions at interfaces between media of different dielectric constants (aqueous solution/polymer matrix). Initially, it was common to believe that the main rejection mechanism in NF was the Donnan exclusion caused by fixed electric charges. That conclusion was based, in fact, on the only observation that double-charge anions were rejected essentially to a greater extent than were single-charge ones. However, that is characteristic of dielectric exclusion, too, and is essentially even more pronounced because the ion-exclusion free energy is proportional to the square of the ion charge (while the Donnan exclusion is linear to it). As a result, for a 1:1 (e.g. HSO_4^- H^+) electrolyte, dielectric exclusion can be much weaker than for

electrolytes with doubly-charge ions 2:1 (e.g. Na_2SO_4) [41]. Table 3 summarises published results on the application of NF membranes in acidic solutions.

Table 3. Comparison of total sulphate rejection data from dilute and concentrated aqueous solutions for various NF membranes.

Name	IEP	Acid	Feed composition C_{H2SO4} (mol/L), pH	Trans-membrane flow, J_v	Rejection (%)	Reference
NF270	3.3 [42]	H_2SO_4	8 wt%	n.a	27%	Tanninen et al. [42]
		H_2SO_4	0.001-0.8 M	n.a.	-5%/ 20%	Tanninen et al. [9]
		H_2SO_4	0.001-0.05	8 µm/s	7-15%	Tanninen et al. [43]
		H_2SO_4	0.0005-0.05	13 µm/s	6-61%	This work
NF20	6.6 [43]	H_2SO_4	0.001-0.05	8 µm/s	3-8%	Tanninen et al. [43]
NF45	7-8 [44]	H_2SO_4	0.001-0.8 M	n.a.	-65%/10%	Tanninen et al. [9]
Desal DK	4 [43]	H_2SO_4	0.001-0.8 M	n.a.	12%	Tanninen et al. [9]
		H_2SO_4	0.001-0.8 M	n.a.	10%/15%	Tanninen et al. [9]
		H_2SO_4	0.1-0.001	8 µm/s	2-40%	Tanninen et al. [43]
		H_2SO_4	0.01-2 M	5-50 $L/m^2 \cdot h$	25-5%	Soldenhoff et al. [45]
Desal KH	4.9 [43]	H_2SO_4	8 wt%	n.a	22%	Tanninen et al. [42]
		H_2SO_4	0.1-0.001	8 µm/s	10-40%	Tanninen et al. [43]
MPF34	-	H_2SO_4	0.01-2	2-22 $L/m^2 \cdot h$	20-10%	Soldenhoff et al. [45]
MPF	-	H_3PO_4 H_2SO_4	28 wt% 1.6 – 2.0 wt%	0.06-0.1 µm/s	<1% 6-1%	Diallo et al. [6]

Rejection values ranged from (slightly) negative up to ca. 40% for all the membranes. Generally, increase in the feed acid concentration resulted in a reduction of the rejection, as demonstrated by Diallo et al. [6]. Their experiments with concentrated mixtures of H_3PO_4/H_2SO_4 (28wt% and 1.8wt%, respectively) showed rejections below 6% for both compounds. In general, the increase of acidity (acid concentration) to values below pH 1 resulted in rejection values below 2–5%, whereas rejection was above 30–40% for dilute solutions of pH above 3, where the dominant species in solution is SO_4^{2-}.

In Figure 6 the total electrolyte rejections determined by Tanninen et al. [43], Pagès et al. [25] and Reig et al. [39] are compared with the results obtained in this work for the pH range from

0.3 to 3 (both studies used sulphuric acid solutions and NF270 membrane). Rejections of sodium sulphate at pH values from 5.75 to 8 are also included for comparison [25].

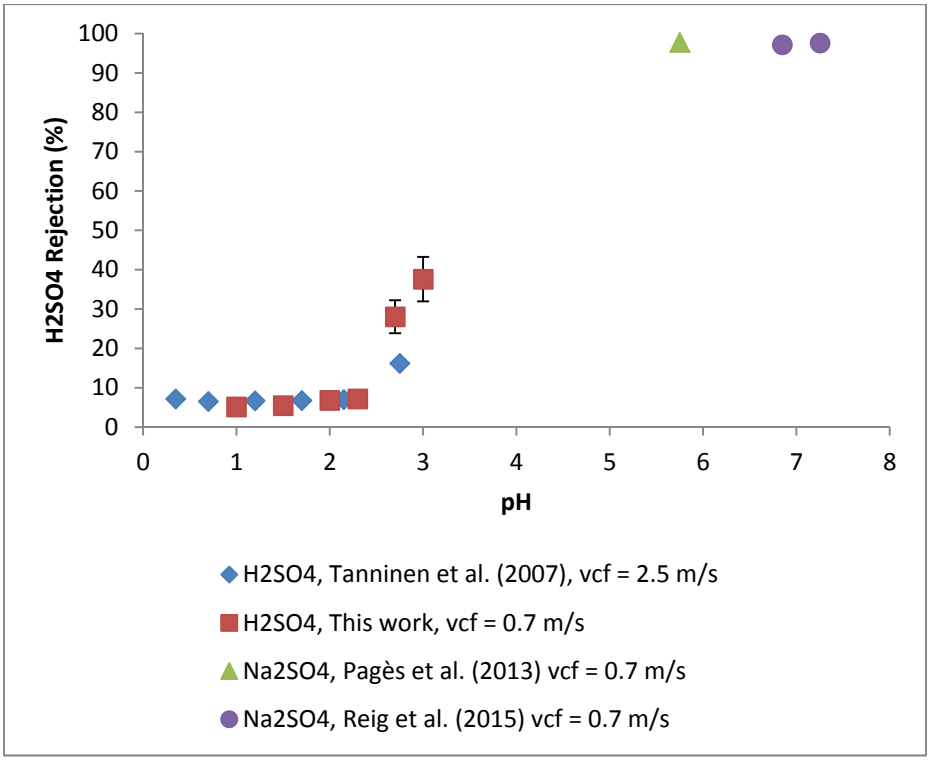

Figure 6 - Comparison of sulphuric rejection as a function of pH for NF270 from this study and from Tanninen et al. [43], Pagès et al. [25] and Reig et al. [39] at trans-membrane volume flux of 8 µm/s.

Both studies reveal similar behaviour, and the total sulphate/sulphuric rejection was approximately constant in the pH range from 0 (with HSO_4^- as predominant species) up to the vicinity of pKa, pH 2.5 (where the concentrations of HSO_4^- and SO_4^{2-} are comparable) with measured rejection values below 8%. Only when pH values were above pKa (pH > pKa + 1), i.e. when more than 90% of the sulphate was present as SO_4^{2-}, did rejection values start to increase from values above 30% at pH 3 to values of >90% for pH values above 5. It should be mentioned that, according to the IEP tests for NF270 in the literature, at pH higher than 3 the membrane becomes negatively charged and most of the carboxylic groups are present in deprotonated form ($RCOO^-$).

Finally, from the measured trans-membrane volume flow values (J_v), the membrane permeability toward water, k_{H2O}, was determined by using Eq. 21:

$$J_v = k_{H2O} \cdot (\Delta P - \Delta\pi) \quad (21)$$

where ΔP is the trans-membrane pressure and Δπ is the osmotic pressure difference across the membrane, assuming the reflection coefficient to be one. Table 4 shows the obtained values for the membrane permeability.

Table 4. Hydraulic membrane permeability values (k_{H2O}) for NF270 membrane with sulphuric and Na_2SO_4 solutions.

pH	C_{SO42-} (ppm)	TMP (bar)	Jv (µm/s)	Total sulphuric rejection, R_{SO42-} (%)	K_{H2O} (µm/(bar·s))	Reference
H_2SO_4 solution						
3	60	4 – 16	13.8 – 53.7	61.6 – 78.5	3.06	This work
2.7	90	4 – 16	13.3 – 53.8	53.3 – 71	3.25	This work
2.3	275	4 – 16	15.4 – 56.9	14 – 38	3.5	This work
2.0	600	4 – 16	14.2 – 53.8	11 – 35	3.3	This work
1.5	2465	4 – 16	12.9 – 48.3	5.8 – 31	3.0	This work
1.0	6030	4 – 16	10.2 – 40.5	5.8 – 30	2.5	This work
Na_2SO_4 solution						
5.8	9600	7 -20	6 – 43	97 – 99	3.1	Pagès et al. [25]
6.9	9600	7 -20	3.9 – 44.5	95 – 99	3.1	Reig et al. [39]
7.3	9600	7 -20	4.3 – 50	96 – 99	3.5	Reig et al. [39]

The membrane hydraulic permeability showed a decrease with the increase of sulphuric concentration (pH decrease). Permeability value is also shown for Na_2SO_4 feed solution; it approached the values for the most dilute sulphuric acid solutions.

4.2. Determination of NF membrane permeances to ions: dependence on solution acidity

The model parameters were membrane ion permeances: equal to the ion permeabilities divided by the active-layer thickness, $P_i^* = P_i/L$. The membrane ion permeances fitted to the experimental data shown in Fig. 5 are listed in Table 5. This presents the results obtained for each experiment (calculated membrane permeances to ion from experimental data, P_i^*) as well as the relative error (given by Eq. 15) obtained when experiments were modelled. The highest deviations from model prediction to experimental data were observed when diluted sulphuric solutions (pH values 3.0 and 2.7) were filtered. At these two pH values, total sulphate ($SO_4^{2-}/HSO_4^-)_t$ rejection started to increase with trans-membrane flow, until reaching a constant value. This behaviour was related to concentration polarisation phenomena, and it was responsible for the deviations between model and experimental data. In order to improve the mathematical model and to predict correctly the transport of a weak electrolyte through the membrane, a correction for concentration polarisation layer should be added.

Table 5. Compilation of membrane permeance to ions (µm/s) of NF270 membrane in sulphuric solutions at 21 ± 1 °C using a cross-flow configuration and cfv of 0.7 m/s.

pH	% HSO_4^-	Calculated membrane permeance to ions, P_i^* (µm/s)			% error
		H^+	SO_4^{2-}	HSO_4^-	
3.0 ± 0.1	10	191.4	0.25	67.1	13.2 %
2.7 ± 0.1	14	200.0	0.15	60.6	12.6 %
2.3 ± 0.1	31	220.0	0.39	149.7	2.5 %
2.0 ± 0.1	48	217.3	0.68	119.0	0.9 %
1.5 ± 0.1	75	220.9	0.32	117.2	1.7 %
1.0 ± 0.1	90	221.6	0.68	118.9	2.7 %

The ion permeance for HSO_4^- was much greater than for SO_4^{2-}, due probably to the dielectric exclusion mechanism as discussed in section 3.1. High values obtained for H^+ can be explained by the high mobility of this ion. Notably, the permeances do not show clear trends in their dependences on pH, which may point to a secondary role played by the membrane fixed charge in this context. However, the potential decrease in the permeances to cations due to the increasing positive fixed charge (with decreasing pH) could be approximately compensated by the increase in the feed ionic strength.

No published studies on the modelling of NF of sulphuric acid solutions at low pH values with the same membrane (NF270) could be found, so our results are compared with sulphate electrolytes in pH-neutral solutions. Permeances to sulphate for two types of strong sulphate electrolytes (Na_2SO_4 and $MgSO_4$) in mixtures of electrolytes as dominant or trace salts are summarised in Table 6. Permeances to SO_4^{2-}, determined by using the SEDF model, ranged from 0.03 to 0.90 µm/s [24,25,39,46] and were similar to the values obtained in this study: 0.15–0.68 µm/s.

Table 6. Compilation of permeance values to SO_4^{2-} (μm/s) to the NF270 membrane in strong sulphate electrolytes as dominant and trace electrolyte at 21 ± 1 °C using cross flow configurations.

Feed composition				cfv (m/s)	J_v (μm/s)	R_{SO42-} (%)	P^*_{SO42-} (μm/s)	Reference
Dominant salt	C_f (mol/L)	Ion trace	C_f (mol/L)					
Sulphate as dominant								
Na_2SO_4	0.1	NaCl	$5{\cdot}10^{-4}$	0.35; 0.7; 1	6 – 43	97 -99	0.05	[25]
Na_2SO_4	0.044	NaCl	$2.2{\cdot}10^{-4}$	1	7 – 93	97 – 99	0.07	[24]
$MgSO_4$	0.1	NaCl	$5{\cdot}10^{-4}$	0.35; 0.7; 1	4.5 – 52	98 – 99	0.05	[25]
$MgSO_4$	0.1	NaCl	$5{\cdot}10^{-4}$	0.7	6 – 48	98 – 99	0.04	[38]
$MgSO_4$	0.1	NH_4Cl	$5{\cdot}10^{-4}$	0.7	4.5 – 47	91 – 98	0.1	[38]
$MgSO_4$	0.1	$NaNO_3$	$5{\cdot}10^{-4}$	0.7	5 – 50	94 – 98	0.03	[38]
$MgSO_4$	0.1	NaI	$5{\cdot}10^{-4}$	0.7	4 – 47	98 -99	0.1	[38]
Sulphate as trace								
NaCl	0.1	$MgSO_4$	0.002	0.35; 0.7; 1	2.5 – 60	97 – 99	0.16	[25]
NaCl	0.088	Na_2SO_4	$2.7{\cdot}10^{-4}$	1	13 – 128	98 – 99	0.13	[24]
NaCl	0.1	$MgSO_4$	$2{\cdot}10^{-3}$	0.7	2 – 60	> 98	0.09	[38]
$MgCl_2$	0.1	Na_2SO_4	$5{\cdot}10^{-4}$	0.7	6 -40	97 -99	0.9	[38]

In addition, just a few studies to determine ion permeances in NF membranes considering reactive transport have been carried out. Niewersch et al. [29,30] studied the application of NF for the recovery of phosphoric acid from the processing of mono-incineration of municipal sewage-sludge bottom ash after leaching with sulphuric acid. Phosphoric/sulphuric solutions, also rich in potassium were treated with an aromatic polyamide membrane (Desal-DL), and the results were modelled by SEDM and accounting for chemical equilibria between species. Desal-DL has an IEP value of 3.0 [47]. High membrane permeances to hydrogen (H^+) were obtained (ranging from 4 to 400 μm/s), while relatively low permeances were obtained for both sulphate species (ranging from 3 to 20 μm/s) [29,30]. Table 7 collects the fitted values of membrane ion permeances of the Desal-DL membrane.

Table 7. Compilation of Desal-DL membrane permeances (μm/s) to H^+ ,HSO_4^- and $SO4^{2-}$ in sulphuric/phosphoric mixtures at 20 ± 1 °C using cross flow configurations and cfv of 0.5 L/min, from Niewersch et al. [29,30]

pH	$[SO_4^{2-}/HSO_4^-]_{TOT}$ (M)	$[K^+]$ (M)	P^*_{H+} (μm/s)	P^*_{SO42-} (μm/s)	P^*_{HSO4-} (μm/s)
1.5	0.150	0.214	4	20	15
2	0.149	0.255	55	4	4
2	0.182	0.318	70	5	3
3	0.153	0.302	400	6	20

According to the reported values, membrane permeances to ion showed a trend in the values of membrane permeances for H^+, in which its value decreased from 400 to 4 μm/s when pH was lowered from 3 to 1.5. However, permeances for HSO_4^- and SO_4^{2-} showed values between 3 to 20 μm/s.

5. Conclusions

Our experimental study of transport of sulphuric solutions within a pH range covering the ratios between SO_4^{2-} and HSO_4^- species from 1:10 to 10:1 revealed strong influence of the speciation on electrolyte rejection. The principal reason for this is the strong dependence of ion permeance of NF membranes on the magnitude of ion charge (probably due to dielectric exclusion).

The experimental data could be quantitatively interpreted by means of the Solution-Electro-Diffusion model extended to account for an equilibrium chemical reaction between the species. An analytical solution of this problem was obtained for the first time.

Although information on the membrane permeances to ions has remained empirical in this study, it can, in principle, be used further for the verification of self-consistency of various mechanistic models. The availability of three 'measurable' quantities: the membrane permeances to these two species (SO_4^{2-}/HSO_4^-) in equilibrium and to H^+, in contrast to just one permeance to the salt available from measurements with strong electrolytes, can make model self-consistency checks much more conclusive. The results indicated that the fitted membrane ion permeances were approximately constant within the studied (acidic) pH range. In the case of sulphate ions, their values were comparable to those determined for the same membrane with strong sulphate electrolytes at neutral pH values.

Nomenclature

c_i	Concentration of component i inside the membrane
c_{ip}	Concentration of component i in permeate side
j_i	Ion flux
J_v	Trans-membrane volume flow
L	Membrane thickness
P_i	Membrane permeability to ion i
P_i^*	Membrane permeance to ion i
pK_a	Acidity constant
x	Dimensionless position in the membrane
z_i	Ion charge
α	Equilibrium dissociation constant
φ	Dimensionless electric potential in the membrane

Acknowledgments

This research was supported by the Waste2Product project (CTM2014-57302-R) financed by the Ministerio de Economía y Competitividad (MINECO) and the Catalan Government (Project Ref. 2014SGR50), Spain. The work of Julio López was supported by the Spanish Ministry (MINECO) within the scope of the grant BES-2015-075051. We also would like to thanks to V. García and J. Ricart for NF270 samples supply and to C. Niewersch for advice exchanage on the computation stage.

Appendix I – Derivation of transport equations for reacting species weak electrolytes

Model development included the following steps:

Step 1) Formulation of the gradient potential from the zero-current flow condition ($\sum_i z_i \cdot j_i = 0$), according to Eq. A1-A2:

$$-\sum z_i \cdot P_i \cdot c_i \cdot \left(\frac{dln\ c_i}{dx} + z_i \cdot \frac{d\varphi}{dx}\right) \rightarrow -\sum z_i^2 \cdot P_i \cdot c_i \cdot \frac{d\varphi}{dx} = \sum z_i \cdot P_i \cdot c_i \cdot \frac{dln\ c_i}{dx} \quad \text{(A1)}$$

$$\frac{d\varphi}{dx} = -\sum \frac{t_i}{z_i} \cdot \frac{dln\ c_i}{dx} \rightarrow \frac{d\varphi}{dx} = -\frac{t_1}{z_1} \cdot \frac{dln\ c_1}{dx} - \frac{t_2}{z_2} \cdot \frac{dln\ c_2}{dx} - \frac{t_3}{z_3} \cdot \frac{dln\ c_3}{dx} \quad \text{(A2)}$$

where t_i represents (Eq. A3):

$$t_i = \frac{z_i^2 \cdot P_i \cdot c_i}{\sum_j z_j^2 \cdot P_j \cdot c_j} \quad \text{(A3)}$$

Step 2) Combination of electro-neutrality condition ($\sum_i z_i \cdot c_i = 0$) and equilibrium condition ($c_3 = \alpha \cdot c_1 \cdot c_2$) to describe concentration of ion 2 (c_2) as a function of the concentration of the other two ions of the weak electrolyte equilibrium (Eq. A6):

$$z_1 \cdot c_1 + z_2 \cdot c_2 + (z_1 + z_2) \cdot \alpha \cdot c_1 \cdot c_2 = 0 \quad \text{(A4)}$$

$$c_2 \cdot (\alpha \cdot c_1 \cdot (z_1 + z_2) + z_2) + z_1 \cdot c_1 = 0 \quad \text{(A5)}$$

$$c_2 = -\frac{z_1 \cdot c_1}{\alpha \cdot c_1 \cdot (z_1 + z_2) + z_2} = -\frac{z_1}{\alpha \cdot (z_1 + z_2) + z_2/c_1} \quad \text{(A6)}$$

Step 3) Definition of the logarithmic concentration gradient of each species in solution (Eq. A7, A13)

Considering the equilibrium condition

$$\frac{dln\ c_3}{dx} = \frac{dln\ c_1}{dx} + \frac{dln\ c_2}{dx} \quad \text{(A7)}$$

Considering the electro-neutrality condition:

$$z_1 \cdot c_1 \cdot \frac{dln\ c_1}{dx} + z_2 \cdot c_2 \cdot \frac{dln\ c_2}{dx} + (z_1 + z_2) \cdot \alpha \cdot c_1 \cdot c_2 \cdot \left(\frac{dln\ c_1}{dx} + \frac{dln\ c_2}{dx}\right) = 0 \quad \text{(A8)}$$

$$\frac{z_1}{c_2} \cdot \frac{dln\ c_1}{dx} + \frac{z_2}{c_1} \cdot \frac{dln\ c_2}{dx} + (z_1 + z_2) \cdot \alpha \cdot \left(\frac{dln\ c_1}{dx} + \frac{dln\ c_2}{dx}\right) = 0 \quad \text{(A9)}$$

$$\frac{dln\ c_1}{dx} \cdot \left(\frac{z_1}{c_2} + \alpha \cdot (z_1 + z_2)\right) + \frac{dln\ c_2}{dx} \cdot \left(\frac{z_2}{c_1} + \alpha \cdot (z_1 + z_2)\right) = 0 \quad \text{(A10)}$$

$$\frac{dln\ c_2}{dx} = -\frac{\frac{z_1}{c_2} + \alpha \cdot (z_1 + z_2)}{\frac{z_2}{c_1} + \alpha \cdot (z_1 + z_2)} \cdot \frac{dln\ c_1}{dx} \quad \text{(A11)}$$

$$c_2 = -\frac{z_1}{\alpha \cdot (z_1 + z_2) + \frac{z_2}{c_1}} \rightarrow \frac{z_1}{c_2} = -\left(\alpha \cdot (z_1 + z_2) + \frac{z_2}{c_1}\right) \quad \text{(A12)}$$

$$\frac{dln\ c_2}{dx} = \frac{\frac{z_2}{c_1}}{\frac{z_2}{c_1} + \alpha \cdot (z_1 + z_2)} \cdot \frac{dln\ c_1}{dx} \quad \text{(A13)}$$

Step 4) Definition of ion flux of component 1 and 2 (Eq.A14-A15):

$$-j_1 = P_1 \cdot c_1 \cdot \left(\frac{dln\ c_1}{dx} + z_1 \cdot \left(-\frac{t_1}{z_1} \cdot \frac{dln\ c_1}{dx} - \frac{t_2}{z_2} \cdot \frac{dln\ c_2}{dx} - \frac{t_3}{z_3} \cdot \frac{dln\ c_3}{dx}\right)\right) \quad \text{(A14)}$$

$$-j_1 = P_1 \cdot c_1 \cdot \left[\frac{dln\ c_1}{dx} \cdot \left(1 - t_1 - \frac{z_1 \cdot t_3}{z_1 + z_2}\right) - \frac{dln\ c_2}{dx} \cdot \left(t_2 \cdot \frac{z_1}{z_2} + \frac{z_1 \cdot t_3}{z_1 + z_2}\right)\right] \quad \text{(A15)}$$

$$-j_2 = P_2 \cdot c_2 \cdot \left[\frac{dln\ c_2}{dx} \cdot \left(1 - t_2 - \frac{z_2 \cdot t_3}{z_1 + z_2}\right) - \frac{dln\ c_1}{dx} \cdot \left(t_1 \cdot \frac{z_2}{z_1} + \frac{z_2 \cdot t_3}{z_1 + z_2}\right)\right] \quad \text{(A16)}$$

Step 5) Taking into account that the difference of ion fluxes of 1 and 2 is conservative, a new equation is obtained (Eq. A17).

$$-J_{\Delta} = P_1 \cdot c_1 \cdot \left[\frac{dln\ c_1}{dx} \cdot \left(1 - t_1 - \frac{z_1 \cdot t_3}{z_1 + z_2}\right) - \frac{dln\ c_2}{dx} \cdot \left(t_2 \cdot \frac{z_1}{z_2} + \frac{z_1 \cdot t_3}{z_1 + z_2}\right)\right] - P_2 \cdot c_2 \cdot \left[\frac{dln\ c_2}{dx} \cdot \left(1 - t_2 - \frac{z_2 \cdot t_3}{z_1 + z_2}\right) - \frac{dln\ c_1}{dx} \cdot \left(t_1 \cdot \frac{z_2}{z_1} + \frac{z_2 \cdot t_3}{z_1 + z_2}\right)\right] \quad \text{(A17)}$$

480

481 By substituting equation A12 in the A17 and rearranging the terms, the equation presented in
482 the section 2 (Eq. 9) could be obtained (A18):

$$J_v L = \frac{\int_{c_{1p}}^{c_{1f}} F(c_1) dc_1}{c_{1p} \cdot \left(1 + \frac{z_1}{c_{1p} \cdot \alpha \cdot (z_1 + z_2) + z_2}\right)} \quad \text{(A18)}$$

483 Where

$$F(c_1) = z_2 \cdot z_3 \cdot \frac{P_1 \cdot (z_2 + c_1 \cdot \alpha \cdot z_3) \cdot (P_2 + P_3 \cdot \alpha \cdot c_1) - P_2 \cdot P_3 \cdot z_1 \cdot \alpha \cdot c_1}{z_2 \cdot (P_2 \cdot z_2 - P_1 \cdot z_1) + c_1 \cdot \alpha \cdot z_3 \cdot (P_3 \cdot z_3 - P_1 \cdot z_1)} \cdot \frac{z_2 + c \cdot \alpha \cdot z_3 - z_1}{(z_2 + c_1 \cdot \alpha \cdot z_3)} \quad \text{(A19)}$$

484 # References

485 [1] K. Liu, Q. Chen, H. Hu, Comparative leaching of minerals by sulphuric acid in a Chinese
486 ferruginous nickel laterite ore, Hydrometallurgy. 98 (2009) 281–286.
487 doi:10.1016/j.hydromet.2009.05.015.

488 [2] A. Agrawal, K.K. Sahu, An overview of the recovery of acid from spent acidic solutions
489 from steel and electroplating industries, J. Hazard. Mater. 171 (2009) 61–75.
490 doi:10.1016/j.jhazmat.2009.06.099.

491 [3] L.L. Tavlarides, J.H. Bae, C.K. Lee, Solvent extraction, membranes, and ion Exchange in
492 hydrometallurgical dilute metals separation, Sep. Sci. Technol. 22 (1987) 581–612.
493 doi:10.1080/01496398708068970.

494 [4] J. Jeong, M.S. Kim, B.S. Kim, S.K. Kim, W.B. Kim, J.C. Lee, Recovery of H2SO4 from waste
495 acid solution by a diffusion dialysis method, J. Hazard. Mater. 124 (2005) 230–235.
496 doi:10.1016/j.jhazmat.2005.05.005.

497 [5] K. Jüttner, U. Galla, H. Schmieder, Electrochemical approaches to environmental
498 problems in the process industry, Electrochim. Acta. 45 (2000) 2575–2594.
499 doi:10.1016/S0013-4686(00)00339-X.

500 [6] H. Diallo, M. Rabiller-Baudry, K. Khaless, B. Chaufer, On the electrostatic interactions in
501 the transfer mechanisms of iron during nanofiltration in high concentrated phosphoric
502 acid, J. Memb. Sci. 427 (2013) 37–47. doi:10.1016/j.memsci.2012.08.047.

503 [7] T.J.K. Visser, S.J. Modise, H.M. Krieg, K. Keizer, The removal of acid sulphate pollution
504 by nanofiltration, Desalination. 140 (2001) 79–86.

505 [8] E. Cséfalvay, V. Pauer, P. Mizsey, Recovery of copper from process waters by
506 nanofiltration and reverse osmosis, Desalination. 240 (2009) 2–6.
507 doi:10.1016/j.desal.2007.11.070.

508 [9] J. Tanninen, M. Mänttäri, M. Nyström, Nanofiltration of concentrated acidic copper

509 sulphate solutions, Desalination. 189 (2006) 92–96. doi:10.1016/j.desal.2005.06.017.

510 [10] M. Nyström, J. Tanninen, M. Mänttäri, Separation of metal sulfates and nitrates from
511 their acids using nanofiltration, Membr. Technol. 2000 (2000) 5–9. doi:10.1016/S0958-
512 2118(00)86633-1.

513 [11] P.K. Eriksson, L.A. Lien, D.H. Green, Membrane technology for treatment of wastes
514 containing dissolved metals, in: V. Ramachandram, C.C. Nesbitt (Eds.), Second Int.
515 Symp. Extr. Process. Treat. Minimization Wastes, 1996: pp. 649–658.

516 [12] M.P. González, R. Navarro, I. Saucedo, M. Avila, J. Revilla, C. Bouchard, Purification of
517 phosphoric acid solutions by reverse osmosis and nanofiltration, Desalination. 147
518 (2002) 315–320. doi:10.1016/S0011-9164(02)00558-1.

519 [13] H.J. Skidmore, K.J. Hutter, Methods of purifying phosphoric acid, US 5945000 A, 1999.
520 https://www.google.es/patents/US5945000?dq=purification+of+aqueous+phosphoric+
521 acid+by+hot+filtration+using+a+polyamide+nanofilter&hl=es&sa=X&ved=0ahUKEwiA8Z
522 2CxKfLAhWDVRQKHYXxCm4Q6AEIHDAA (accessed March 4, 2016).

523 [14] S. Bason, Y. Kaufman, V. Freger, Analysis of ion transport in nanofiltration using
524 phenomenological coefficients and structural characteristics, J. Phys. Chem. B. 114
525 (2010) 3510–3517. doi:10.1021/jp911615n.

526 [15] J. Schaep, B. Van der Bruggen, C. Vandecasteele, D. Wilms, Influence of ion size and
527 charge in nanofiltration, Sep. Purif. Technol. 14 (1998) 155–162. doi:10.1016/S1383-
528 5866(98)00070-7.

529 [16] A.E. Yaroshchuk, Rejection of single salts versus transmembrane volume flow in RO/NF:
530 thermodynamic properties, model of constant coefficients, and its modification, J.
531 Memb. Sci. 198 (2002) 285–297. doi:10.1016/S0376-7388(01)00668-8.

532 [17] K.S. Spiegler, O. Kedem, Thermodynamics of hyperfiltration (reverse osmosis): criteria
533 for efficient membranes, Desalination. 1 (1966) 311–326.

534 [18] D.W. Nielsen, G. Jonsson, Bulk-Phase criteria for negative ion rejection in nanofiltration
535 of multicomponent salt solutions, Sep. Sci. Technol. 29 (1994) 1165–1182.
536 doi:10.1080/01496399408005623.

537 [19] W.R. Bowen, J.S. Welfoot, P.M. Williams, Linearized transport model for nanofiltration:
538 Development and assessment, AIChE J. 48 (2002) 760–773. doi:10.1002/aic.690480411.

539 [20] W.R. Bowen, H. Mukhtar, Characterisation and prediction of separation performance of
540 nanofiltration membranes, J. Memb. Sci. 112 (1996) 263–274. doi:10.1016/0376-
541 7388(95)00302-9.

542 [21] J. Garcia-Aleman, J.M. Dickson, Mathematical modeling of nanofiltration membranes
543 with mixed electrolyte solutions, J. Memb. Sci. 235 (2004) 1–13.
544 doi:10.1016/j.memsci.2003.11.023.

545 [22] A. Yaroshchuk, X. Martínez-Lladó, L. Llenas, M. Rovira, J. de Pablo, J. Flores, P. Rubio,
546 Mechanisms of transfer of ionic solutes through composite polymer nano-filtration
547 membranes in view of their high sulfate/chloride selectivities, Desalin. Water Treat. 6
548 (2009) 48–53.

549 [23] A. Yaroshchuk, M.L. Bruening, E.E. Licón Bernal, Solution-Diffusion-Electro-Migration

model and its uses for analysis of nanofiltration, pressure-retarded osmosis and forward osmosis in multi-ionic solutions, J. Memb. Sci. 447 (2013) 463–476. doi:10.1016/j.memsci.2013.07.047.

[24] A. Yaroshchuk, X. Martínez-Lladó, L. Llenas, M. Rovira, J. de Pablo, Solution-diffusion-film model for the description of pressure-driven trans-membrane transfer of electrolyte mixtures: One dominant salt and trace ions, J. Memb. Sci. 368 (2011) 192–201. doi:10.1016/j.memsci.2010.11.037.

[25] N. Pages, A. Yaroshchuk, O. Gibert, J.L. Cortina, Rejection of trace ionic solutes in nanofiltration : Influence of aqueous phase composition, Chem. Eng. Sci. 104 (2013) 1107–1115. doi:10.1016/j.ces.2013.09.042.

[26] R. Fornarelli, M. Mullett, D. Ralph, Factors influencing nanofiltration of acid mine drainage, Reliab. Mine Water Technol. (2013) 563–568.

[27] O. Nir, L. Ophek, O. Lahav, Acid-base dynamics in seawater reverse osmosis: experimental evaluation of a reactive-transport algorithm, Environ. Sci. Water Res. Technol. 2 (2015) 107–116. doi:10.1039/C5EW00228A.

[28] O. Nir, N.F. Bishop, O. Lahav, V. Freger, Modeling pH variation in reverse osmosis, Water Res. 87 (2015) 328–335. doi:10.1016/j.watres.2015.09.038.

[29] C. Niewersch, A.L.B. Bloch, S. Yüce, T. Melin, M. Wessling, Nanofiltration for the recovery of phosphorus — Development of a mass transport model, Desalination. 346 (2014) 70–78. doi:10.1016/j.desal.2014.05.011.

[30] C. Niewersch, Nanofiltration for phosphorus recycling from sewage sludge, Verlagshaus Mainz GmbH, 2013.

[31] E. Idil Mouhoumed, A. Szymczyk, A. Schäfer, L. Paugam, Y.H. La, Physico-chemical characterization of polyamide NF/RO membranes: Insight from streaming current measurements, J. Memb. Sci. 461 (2014) 130–138. doi:10.1016/j.memsci.2014.03.025.

[32] W.J. Koros, G.K. Fleming, S.M. Jordan, T.H. Kim, H.H. Hoehn, Polymeric membrane materials for solution-diffusion based permeation separations, Prog. Polym. Sci. 13 (1988) 339–401. doi:10.1016/0079-6700(88)90002-0.

[33] S.H. Kim, S.-Y. Kwak, T. Suzuki, Evidence to demonstrate the flux-enhancement mechanism in morphology-controlled thin-film-composite (TFC)membrane, Environ. Sci. Technol. 39 (2005) 1764–1770.

[34] O. Coronell, M.I. González, B.J. Mariñas, D.G. Cahill, Ionization behavior, stoichiometry of association, and accessibility of functional groups in the active layers of reverse osmosis and nanofiltration membranes, Environ. Sci. Technol. 44 (2010) 6808–6814. doi:10.1021/es100891r.

[35] G. Artuğ, I. Roosmasari, K. Richau, J. Hapke, A Comprehensive Characterization of Commercial Nanofiltration Membranes, Sep. Sci. Technol. 42 (2007) 2947–2986. doi:10.1080/01496390701560082.

[36] O. Coronell, B.J. Mariñas, D.G. Cahill, Depth heterogeneity of fully aromatic polyamide active layers in reverse osmosis and nanofiltration membranes, Environ. Sci. Technol. 45 (2011) 4513–4520. doi:10.1021/es200007h.

[37] I. Puigdomenech, Chemical equilibirum software Hydra/Medusa, (2001). https://sites.google.com/site/chemdiagr/home.

[38] N. Pagès, M. Reig, O. Gibert, J.L. Cortina, Trace ions rejection tunning in NF by selecting solution composition: Ion permeances estimation, Chem. Eng. J. 308 (2017) 126–134. doi:10.1016/j.cej.2016.09.037.

[39] M. Reig, N. Pagès, E. Licon, C. Valderrama, O. Gibert, A. Yaroshchuk, J.L. Cortina, Evolution of electrolyte mixtures rejection behaviour using nanofiltration membranes under spiral wound and flat-sheet configurations, Desalin. Water Treat. 56 (2015) 3519–3529. doi:10.1080/19443994.2014.974215.

[40] M. Mullett, R. Fornarelli, D. Ralph, Nanofiltration of mine water: impact of feed pH and membrane charge on resource recovery and water discharge, Membranes (Basel). 4 (2014) 163–180. doi:10.3390/membranes4020163.

[41] A.E. Yaroshchuk, Dielectric exclusion of ions from membranes, Adv. Colloid Interface Sci. 85 (2000) 193–230. doi:10.1016/S0001-8686(99)00021-4.

[42] J. Tanninen, S. Platt, A. Weis, M. Nyström, Long-term acid resistance and selectivity of NF membranes in very acidic conditions, J. Memb. Sci. 240 (2004) 11–18. doi:10.1016/j.memsci.2004.04.006.

[43] J. Tanninen, M. Mänttäri, M. Nyström, Effect of electrolyte strength on acid separation with NF membranes, J. Memb. Sci. 294 (2007) 207–212. doi:10.1016/j.memsci.2007.02.042.

[44] S. Szoke, G. Patzay, L. Weiser, Characteristics of thin-film nanofiltration membranes at various pH-values, Desalination. 151 (2003) 123–129. doi:10.1016/S0011-9164(02)00990-6.

[45] K. Soldenhoff, J. Mcculloch, A. Manis, P. Macintosh, Nanofiltration in metal and acid recovery, in: Nanofiltration - Princ. Appl., 2005: pp. 460–478.

[46] N. Fridman-Bishop, O. Nir, O. Lahav, V. Freger, Predicting the rejection of major seawater ions by spiral-wound nanofiltration membranes, Environ. Sci. Technol. 49 (2015) 8631–8638. doi:10.1021/acs.est.5b00336.

[47] A.I.C. Morão, A.M. Brites Alves, M.D. Afonso, Concentration of clavulanic acid broths: Influence of the membrane surface charge density on NF operation, J. Memb. Sci. 281 (2006) 417–428. doi:10.1016/j.memsci.2006.04.010.